# Local variations of the magnetization effected by an external field in molecular rings

N. P. Konstantinidis
*Mathematics and Science Department, American University in Bulgaria,*
*Sv. Buchvarova Str. 8, Blagoevgrad 2700, Bulgaria*
(Dated: May 15, 2025)

It is shown that an external magnetic field generates local variations of the classical ground-state magnetization in molecular rings of antiferromagnetic icosahedra with isotropic spin interactions. The magnetic response is characterized by a multitude of magnetization discontinuities occurring across the ring. In addition, a parity effect with respect to the number of icosahedra allows for magnetization jumps that occur at different field values for different molecules and produce an even more pronounced local variation of the magnetization. It is also found that for specific field ranges all canting angles of the molecular magnetizations increase with the field. These findings are in sharp contrast with the ones for rings of individual spins.

## I. INTRODUCTION

In frustrated magnetic systems competing interactions lead to a wide range of unconventional phenomena at the classical and quantum level [1, 2]. These occur even in the absence of magnetic anisotropy, as is the case with the isotropic nearest-neighbor antiferromagnetic Heisenberg model (AHM) [3–7]. Apart from extended systems, finite units whose connectivity is associated with frustrated interactions are of particular importance. These include the icosahedral-symmetry Platonic solids [8–14], the icosahedron and the dodecahedron, which have been found to support nontrivial magnetic states at the classical and quantum level [15–29]. Furthermore, the introduction of an external field leads to discontinuous magnetic response in the absence of magnetic anisotropy.

The above properties of the icosahedral Platonic solids are the motivation to consider rings of icosahedra, with their magnetic properties modeled by the classical AHM. Classical spins forming rings and interacting according to the AHM have an increasing external field turn them toward and eventually align with its direction. In this way the so-called umbrella configuration is realized, in which all the spins form the same angle with the field [30–32]. Here the magnetic units forming a ring are taken to be the total magnetizations of the icosahedra. The interactions within an icosahedron and between neighboring ones are taken to be antiferromagnetic. They lead to a zero-field ground state where each molecule has no residual magnetization if their number is a multiple of three. This number does not introduce additional frustration over the one of a single molecule, as neighboring spins form the same angle in the ground state as in an isolated icosahedron. Furthermore, interacting spins belonging to neighboring molecules are antiparallel. As the field is switched on each molecule develops a finite magnetization which increases with the field, in contrast to a single isolated spin in a ring that has a fixed magnetization.

The classical total magnetization of an isolated icosahedron has a discontinuity in an external field [18]. Here it is found that in a ring of icosahedra an external field generates multiple distinct ground states separated by magnetization jumps. Many of them break translational symmetry with respect to the magnitude of the magnetization unit, unlike the case of a ring of spins, with different icosahedra having different magnetization magnitude. In addition the angles between these magnetizations and the external field are not the same. The result is magnetization projections along the field axis which are also different. Furthermore, all the polar angles increase simultaneously as a function of the field for specific field ranges. This is in contrast with the variation of the polar angles in the umbrella state of a ring of spins, where all decrease with the field. Even in an isolated icosahedron, where polar angles of individual spins increase for a specific field range, this can not happen for all simultaneously [33].

More specifically, in rings of three and six icosahedra magnetization discontinuities lead to ground states where the magnetization varies locally. For a three-membered ring all molecular magnetizations and their polar angles can be different. For six icosahedra the molecules can share magnetizations and polar angles in pairs, or even in two groups of two and four molecules. In addition a parity effect is observed with respect to the number of molecules being an odd or even multiple of three. In the former case the magnetization discontinuity that corresponds to an isolated icosahedron is split in two, first occurring for one molecule with the other two following at a higher field. This results in a more pronounced local variation of the magnetization as a function of the external field and points to a difference in the magnetic behavior between rings with an even and an odd number of molecules, similarly to the case of rings of individual spins. Such a split is absent for the six-membered ring. On the other hand, for six icosahedra a susceptibility discontinuity close to saturation leads to complete alignment of the magnetizations of the icosahedra with the field. Further increasing the field results only in bigger magnetizations until they are maximized at the saturation field.

Due to computational requirements rings of more than six icosahedra have not been considered. It is an open question how the magnetic response develops going toward the thermodynamic limit, how the lowest-energy configurations evolve, and if more discontinuities emerge.

The calculations in this paper are relevant to icosahedral quasicrystals and their approximant crystals [34–38]. Going from one to three-dimensional structures the results of this paper may survive in one form or another.

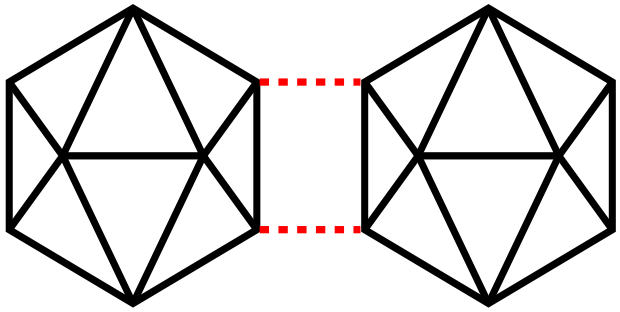

FIG. 1: Planar projection of two interacting icosahedra. The (black) solid lines correspond to bonds within the same icosahedron with exchange interaction value $cos\omega$, while the (red) dashed lines to neighboring-icosahedra bonds with exchange interaction value $sin\omega$.

The plan of this paper is as follows: in Sec. II the AHM in a magnetic field is introduced for a ring of icosahedra, and in Sec. III its ground state is calculated for a ring of three icosahedra. Sec. IV extends the results to a ring of six molecules, and finally Sec. V presents the conclusions.

## II. MODEL

The icosahedron is made of 12 equivalent vertices and 20 identical triangles [8]. It has the symmetry of the icosahedral $I_h$ group, the biggest point-symmetry group with 120 symmetry operations [39]. Here a ring of $N$ icosahedra is considered and the total number of vertices is $12N$. In each icosahedron a classical spin $\vec{s}_{ij}$, $i = 1, 2, \ldots, N$, $j = 1, 2, \ldots, 12$ of unit magnitude is mounted on each of its vertices. The interactions within each icosahedron follow its connectivity, while nearest-neighbor icosahedra interact via the two pairs of spins of their closest edges (Fig. 1). Periodic boundary conditions are assumed. The Hamiltonian of the isotropic nearest-neighbor AHM in a magnetic field $\vec{h}$ describes the interactions between the spins. They are parametrized with $\omega$, with $cos\omega$ the interactions between spins in the same icosahedron and $sin\omega$ the ones between spins belonging to different icosahedra. The Hamiltonian is:

$$H = cos\omega \sum_{i=1}^{N} \sum_{<jk>} \vec{s}_{ij} \cdot \vec{s}_{ik} + sin\omega \sum_{i=1}^{N} \sum_{<jk>'} \vec{s}_{ij} \cdot \vec{s}_{i+1k} - h \sum_{i=1}^{N} \sum_{j=1}^{12} s_{ij}^{z} \quad (1)$$

The brackets indicate that interactions are nonzero only between nearest neighbors. The icosahedral ring has $30N$ bonds of type $cos\omega$ and $2N$ bonds of type $sin\omega$. The magnetic field points along the $z$ axis. To ensure that the zero-field ground state has nearest-neighbors in the same icosahedron with energy $-\frac{\sqrt{5}}{5}$ as in an isolated molecule [17] and in different icosahedra antiparallel, $N$ is taken to be a multiple of 3. In this way no extra frustration is added by assembling together the icosahedra.

The lowest-energy configuration was calculated numerically as a function of the magnetic field [15, 20, 40]. For a specific field the initial spin configuration is selected by assigning random values to the polar and azimuthal angles of the spins. Then each angle is moved opposite the direction of its gradient, until the energy is minimized. To ensure that the global lowest-energy configuration is found this procedure is repeated for a sufficient number of different random initial configurations.

## III. RING OF THREE ICOSAHEDRA

The zero-field ground state of Hamiltonian (1) on an isolated icosahedron has all nearest-neighbor correlations equal to $-\frac{\sqrt{5}}{5}$ [17]. The introduction of an external field leads to a magnetization discontinuity as the field is ramped up [18]. Such a discontinuity is not expected in the absence of magnetic anisotropy and originates from the frustrated connectivity of the molecule.

The minimum number of icosahedra forming a ring with no extra frustration from the one of an isolated molecule is $N = 3$. In a ring of icosahedra the magnetic units are taken to be the total magnetizations of the individual icosahedra $\vec{M}_i$, with each forming a polar angle $\theta_i$ with the field. The triangle of icosahedra is contrasted with one of single spins, perhaps the simplest frustrated unit. In the ground state of Hamiltonian (1) on the triangle the magnetic field turns the spins toward its direction, with each spin forming the same angle with the field.

Figure 2 plots the total ground-state magnetization along the field $M^z$ of Hamiltonian (1) for $\omega = \frac{\pi}{10}$. The introduction of intermolecular bonds results in new magnetization discontinuities (Table I). The single icosahedron discontinuity is flanked by a new one on either side. A lower-field jump also appears, bringing the total number of discontinuities to four.

At zero field each icosahedron has zero magnetization. When the field is switched on the icosahedra acquire a common finite $M_i$, emerging for each one at the finite polar angle $\theta_i = 1.818 \times 10^{-3}\pi$ as $h \to 0$ (Fig. 3). For low magnetic fields the $M_i$ form the same polar angle with the $z$ axis, resembling a triangle of spins. The common polar angle is small and at first decreases with the field, achieving a local minimum at $\frac{h}{h_{sat}} = 0.178$. However, in contrast to what happens for a ring of spins, for higher fields this angle increases. This is also in contrast with the polar angles of an isolated icosahedron, where not all of them can be increasing functions of $h$, even for a short field range [33]. Still the projections of the molecular

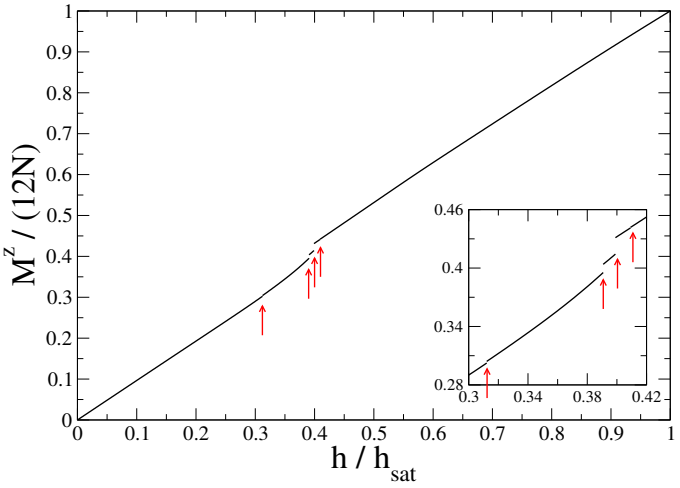


FIG. 2: Magnetization per spin $\frac{M^z}{12N}$ along the field as a function of the magnetic field over its saturation value $\frac{h}{h_{sat}}$ in the ground state of Hamiltonian (1) for a ring of $N = 3$ icosahedra for $\omega = \frac{\pi}{10}$. The (red) solid arrows point at the locations of the magnetization discontinuities.

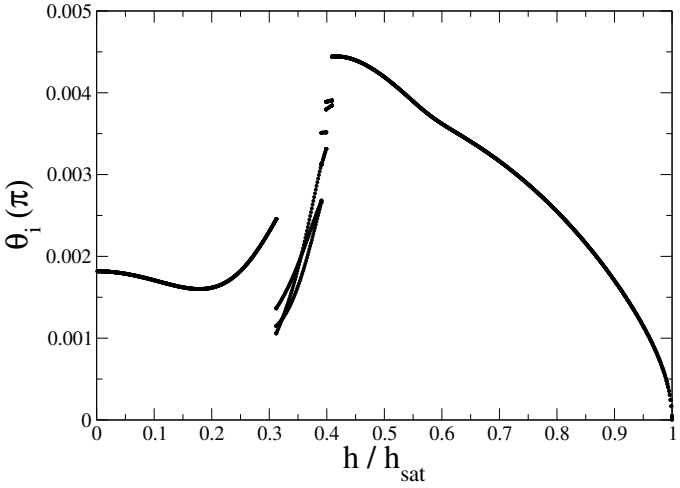


FIG. 3: Polar angles $\theta_i$ of the magnetizations of the icosahedra $M_i$ as a function of the magnetic field over its saturation value $\frac{h}{h_{sat}}$ in the ground state of Hamiltonian (1) for a ring of $N = 3$ icosahedra for $\omega = \frac{\pi}{10}$.

TABLE I: Ground-state magnetization discontinuities of Hamiltonian (1) for a triangle of icosahedra ($N = 3$) and $\omega = \frac{\pi}{10}$. The columns give the magnetic field over the saturation field $\frac{h}{h_{sat}}$ for which the discontinuities occur, the total magnetization along the field just below and just above the discontinuity over the number of sites $12N$, and the corresponding strength of the magnetization jumps.

| $\frac{h}{h_{sat}}$ | $(\frac{M^z}{12N})_-$ | $(\frac{M^z}{12N})_+$ | $\frac{\Delta M^z}{12N}$ $(\times 10^{-3})$ |
|---|---|---|---|
| 0.31214447 | 0.30243210 | 0.30412411 | 1.69201 |
| 0.390745820 | 0.39535993 | 0.40383713 | 8.47720 |
| 0.398995468 | 0.41428942 | 0.43122713 | 16.93771 |
| 0.40916029 | 0.44123730 | 0.44174704 | 0.50974 |

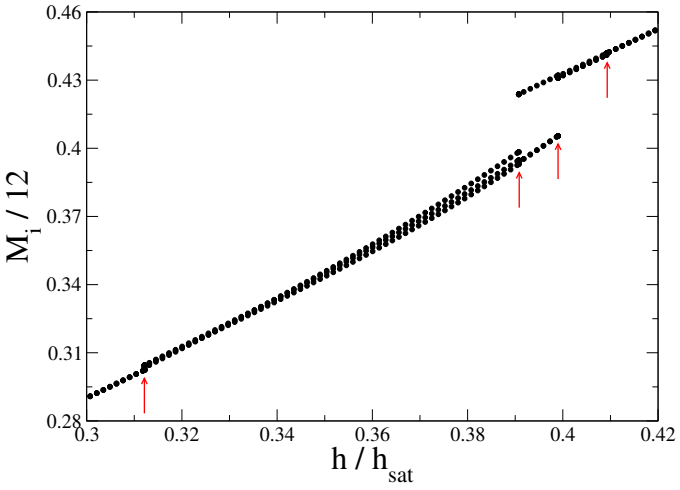


FIG. 4: Magnitude of the total magnetization per spin $\frac{M_i}{12}$ of each icosahedron $i = 1, 2, 3$ as a function of the magnetic field over its saturation value $\frac{h}{h_{sat}}$ in the ground state of Hamiltonian (1) for a ring of $N = 3$ icosahedra for $\omega = \frac{\pi}{10}$. The (red) solid arrows point at the locations of the magnetization discontinuities.

magnetizations along the $z$ axis $M_i^z$ are getting bigger with the field as expected and are equal to $\frac{M^z}{N}$, since the $M_i$ increase with $h$ for each icosahedron, compensating for the bigger polar angles.

At $\frac{h}{h_{sat}} = 0.31214447$ the first magnetization discontinuity occurs (Fig. 2 and Table I). It leads to a ground state where each icosahedron has its own $M_i$ (Fig. 4). Fig. 5 plots the standard deviation of the $M_i$. The angles they form with the field are different (Fig. 6) and the $M_i^z$ are also different. This lowest-energy configuration is again in contrast with the umbrella state of a triangle of spins. Furthermore, the polar angles keep getting bigger with the field. Fig. 7 shows the projection of the total magnetization per spin along the field for the spins that do not participate in intermolecular bonds, and for the ones that do. The value for the latter decreases at the jump.

The next magnetization discontinuity occurs at $\frac{h}{h_{sat}} =$ 0.390745820, with the change in $M^z$ significantly bigger than the one of the first jump (Table I). Now two icosahedra share the $M_i$ and its polar angle, with the remaining one having bigger values for both (Figs 4 and 6). The icosahedron with the bigger $M_i$ has undergone a jump similar to the one of an isolated icosahedron. This is attested by the strength of the jump and the discontinuity field, both very close in value to the ones of the isolated icosahedron [18]. The ring of icosahedra has locally two distinct $M_i$ differing in value in a more pronounced way,

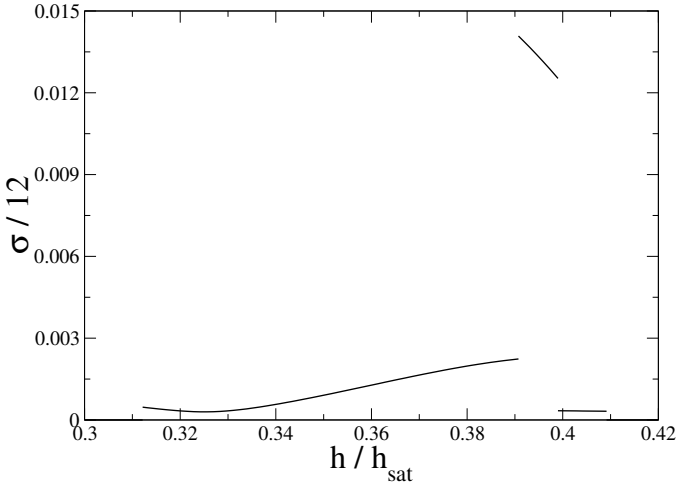


FIG. 5: Standard deviation $\sigma$ of the magnitude of the molecular magnetization per spin $\frac{M_i}{12}$ as a function of the magnetic field over its saturation value $\frac{h}{h_{sat}}$ in the ground state of Hamiltonian (1) for a ring of $N = 3$ icosahedra for $\omega = \frac{\pi}{10}$.

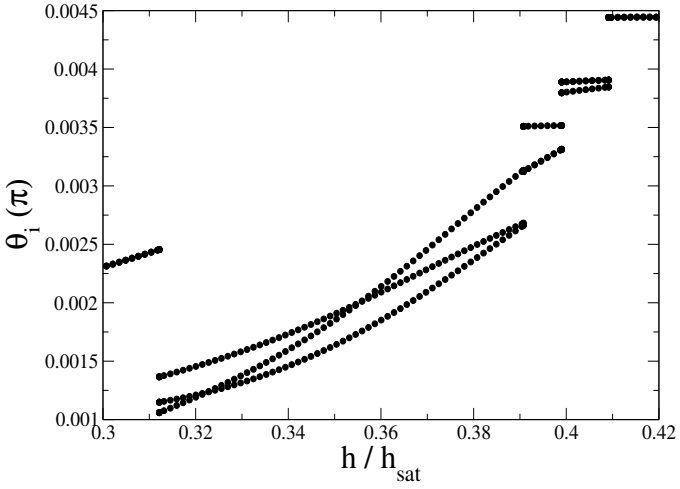


FIG. 6: Part of Fig. 3 in greater detail.

with the individual icosahedra being on different sides of the magnetization jump of an isolated icosahedron. The standard deviation of the $M_i$ acquires now maximum values (Fig. 5).

At the next magnetization discontinuity, which occurs at $\frac{h}{h_{sat}} = 0.398995468$, the other two $M_i$ undergo the jump that corresponds to the one of the isolated icosahedron. This results in a discontinuity value twice as big as the previous one (Table I). The number of distinct magnetizations is still two, but the standard deviation of the $M_i$ becomes smaller (Fig. 5). The icosahedron with the bigger magnetization forms the smallest polar angle with the field.

Following a discontinuity weak in strength at $\frac{h}{h_{sat}} = 0.40916029$ all the icosahedra acquire the same $M_i$, with

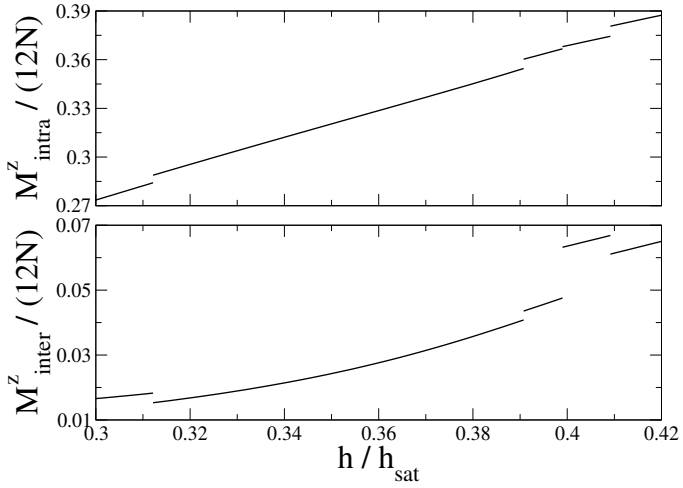


FIG. 7: Total magnetization per spin along the field of the spins that participate in intericosahedral bonds $M^z_{inter}$ and the ones that do not $M^z_{intra}$ as a function of the magnetic field over its saturation value $\frac{h}{h_{sat}}$ in the ground state of Hamiltonian (1) for a ring of $N = 3$ icosahedra for $\omega = \frac{\pi}{10}$.

each one forming the same angle with the field all the way to saturation. The spins that participate in intermolecular bonds again decrease their total magnetization along the field at this jump (Fig. 7). The polar angle with the field keeps increasing up to $\frac{h}{h_{sat}} = 0.417$, but this is again compensated from the rise of the $M_i$ to result in $M^z_i$ that increase with the field.

The above results show that an external field generates locally different $M_i$ for specific field ranges. The three-icosahedron ring is magnetically acting as being made of more than one parts. Each part reacts differently to the field, hosting distinctly different magnetic configurations that locally change by ramping up the field. Furthermore, the magnetization jump of a single icosahedron is distributed in two clear-cut jumps in the three-molecule ring, with the change in the total magnetization (Fig. 2) localized to one or two individual molecules in each jump.

## IV. RING OF SIX ICOSAHEDRA

The next-bigger ring of icosahedra with zero-field intramolecular correlations equal to the ones of an isolated icosahedron and nearest-neighbor spins belonging to different icosahedra antiparallel is a hexagon. Figure 8 shows the total ground-state magnetization along the field $M^z$ of Hamiltonian (1) for $\omega = \frac{\pi}{10}$. The total number of magnetization discontinuities in a field is now six, and close to saturation the susceptibility is also discontinuous (Table II).

An infinitesimal field generates a ground-state magnetization $M_i$ for each icosahedron at a polar angle with the field equal to $1.818 \times 10^{-3}\pi$ (Fig. 9), the same with the one of $N = 3$. The common polar angle decreases

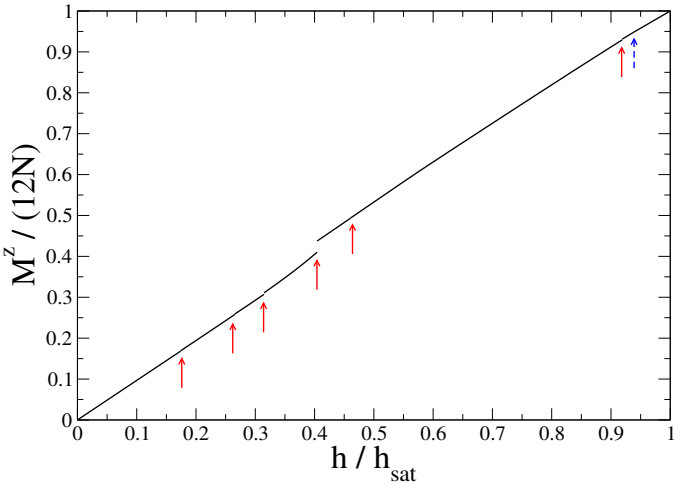


FIG. 8: Reduced magnetization $\frac{M^z}{12N}$ along the field as a function of the magnetic field over its saturation value $\frac{h}{h_{sat}}$ in the ground state of Hamiltonian (1) for a ring of $N = 6$ icosahedra for $\omega = \frac{\pi}{10}$. The (red) solid arrows point at the locations of the magnetization discontinuities. The (blue) dashed arrow points at the location of the susceptibility discontinuity.

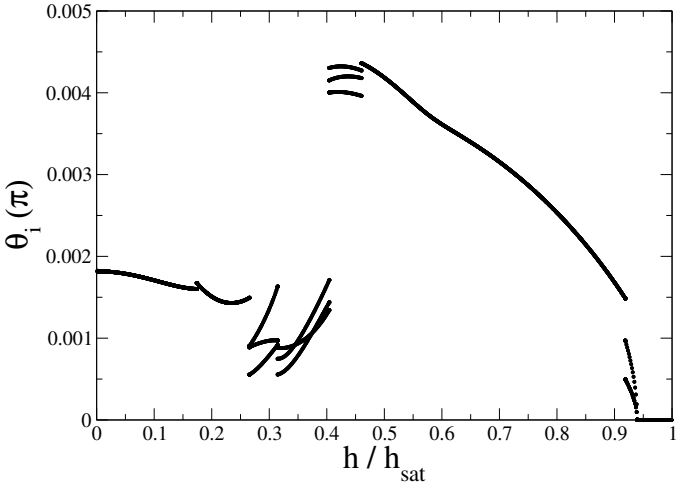


FIG. 9: Polar angles $\theta_i$ of the magnetizations of the icosahedra $M_i$ as a function of the magnetic field over its saturation value $\frac{h}{h_{sat}}$ in the ground state of Hamiltonian (1) for a ring of $N = 6$ icosahedra for $\omega = \frac{\pi}{10}$.

TABLE II: Ground-state magnetization discontinuities of Hamiltonian (1) for a triangle of icosahedra ($N = 6$) and $\omega = \frac{\pi}{10}$. The columns give the magnetic field over the saturation field $\frac{h}{h_{sat}}$ for which the discontinuities occur, the total magnetization along the field just below and just above the discontinuity over the number of sites $12N$, and the corresponding strength of the magnetization jumps. A susceptibility discontinuity occurs at $\frac{h}{h_{sat}} = 0.93948$, where the value of the magnetization is 0.94913.

| $\frac{h}{h_{sat}}$ | $(\frac{M}{12N})_-$ | $(\frac{M}{12N})_+$ | $\frac{\Delta M}{12N}$ $(\times 10^{-3})$ |
|---|---|---|---|
| 0.17405567 | 0.16827873 | 0.16907497 | 0.79624 |
| 0.2655524 | 0.2579651 | 0.2591112 | 1.1461 |
| 0.3146333 | 0.3070018 | 0.3108143 | 3.8125 |
| 0.404314 | 0.4103450 | 0.4375794 | 27.2344 |
| 0.4604222 | 0.4930904 | 0.4934528 | 0.3624 |
| 0.918823548 | 0.92918918 | 0.93102521 | 1.83603 |

with the field. At $\frac{h}{h_{sat}} = 0.17405567$ a magnetization jump occurs, leading to a lowest-energy configuration with a higher common polar angle. The polar angle then decreases with the field but reaches a minimum at $\frac{h}{h_{sat}} = 0.234$ and then the $M_i$ turn away from the field.

A new jump in the magnetization occurs at $\frac{h}{h_{sat}} = 0.2655524$. Following it translational symmetry is broken, with the icosahedra sharing $M_i$ (Fig. 10) and polar angle values (Fig. 11) in pairs. Two of the pairs are adjacent to each other. Fig. 12 shows the standard deviation of the $M_i$. The polar angles mostly increase with the field. The projections of the molecular magnetizations along the field $M_i^z$ follow the pattern of the $M_i$ and their polar angles.

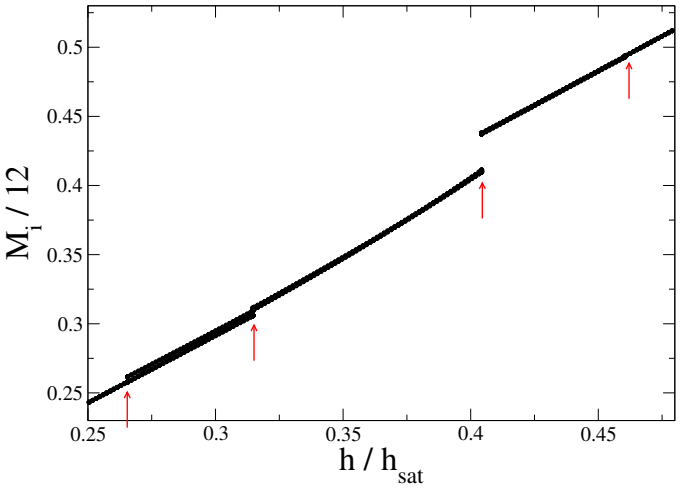


FIG. 10: Magnitude of the total magnetization per spin $\frac{M_i}{12}$ of each icosahedron $i = 1, 2, \ldots, 6$ as a function of the magnetic field over its saturation value $\frac{h}{h_{sat}}$ in the ground state of Hamiltonian (1) for a ring of $N = 6$ icosahedra for $\omega = \frac{\pi}{10}$. The (red) solid arrows point at the locations of the magnetization discontinuities.

The next magnetization jump occurs at $\frac{h}{h_{sat}} = 0.3146333$. The lowest-energy configuration does not change. The polar angles increase with the field and the standard deviation of the $M_i$ is now smaller. This discontinuity occurs at a field very close to the one of the first discontinuity of $N = 3$ and has similar characteristics with it (Sec. III).

The next discontinuity occurs at $\frac{h}{h_{sat}} = 0.404314$ and the lowest-energy configuration is still the same. Each

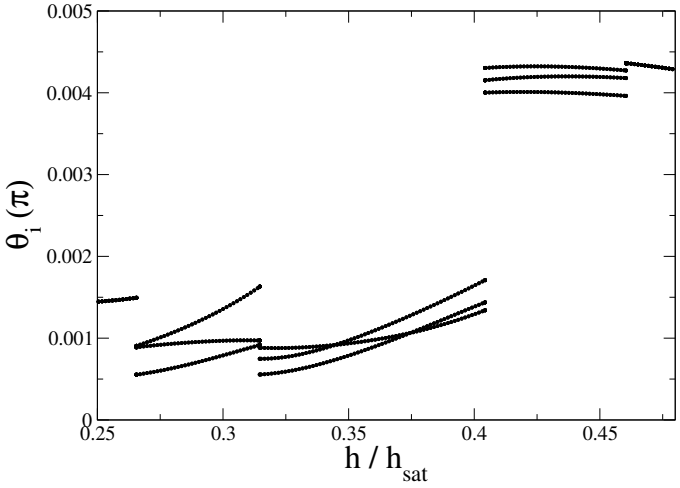


FIG. 11: Part of Fig. 9 in greater detail.

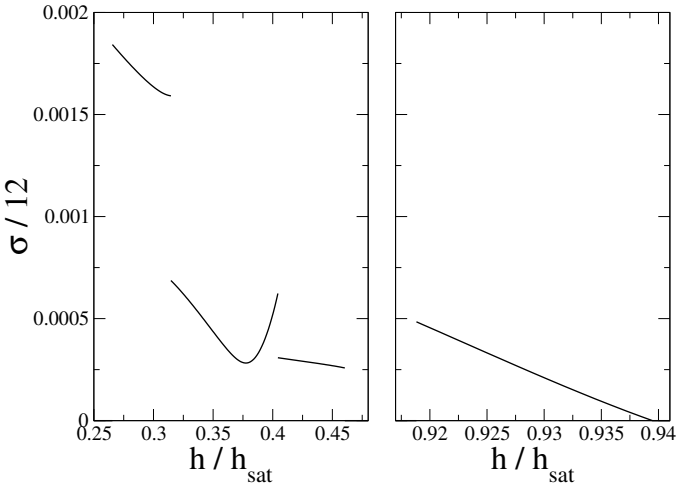


FIG. 12: Standard deviation $\sigma$ of the magnitude of the molecular magnetization per spin $\frac{M_i}{12}$ as a function of the magnetic field over its saturation value $\frac{h}{h_{sat}}$ in the ground state of Hamiltonian (1) for a ring of $N = 6$ icosahedra for $\omega = \frac{\pi}{10}$.

$M_i^z$ undergoes the magnetization jump of the isolated icosahedron, with the corresponding field value very close to the one of an isolated molecule [18]. This is in contrast with what happens for $N = 3$, where the isolated-icosahedron jump occurs at different fields for different molecules. At this jump the increase in the magnetization allows the polar angles to increase.

Above a magnetization jump at $\frac{h}{h_{sat}} = 0.4604222$ all $M_i$ and polar angles become equal. The $M_i$ turn toward the field but at the last discontinuity at $\frac{h}{h_{sat}} = 0.918823548$ their translational symmetry is again lost. Two distinct $M_i$ occur now in the ground state, with groups of four and two icosahedra sharing the $M_i$ value (Fig. 13) as well as the polar angle (Fig. 14), providing another way to break the translational symmetry. The two icosahedra that share one of the $M_i$ values are maximally distanced from one another. Following a susceptibility discontinuity at $\frac{h}{h_{sat}} = 0.93948$ all $M_i$ align with the field, even though saturation has not been reached yet. Further increasing the field results in higher $M_i$'s up to saturation.

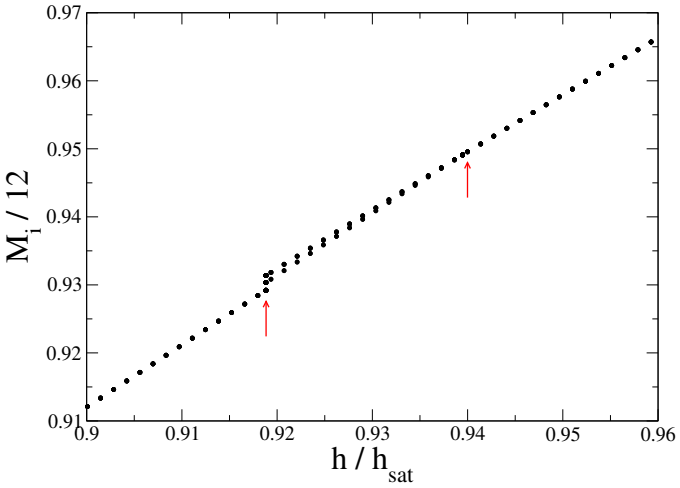


FIG. 13: Same as Fig. 10 but close to saturation.

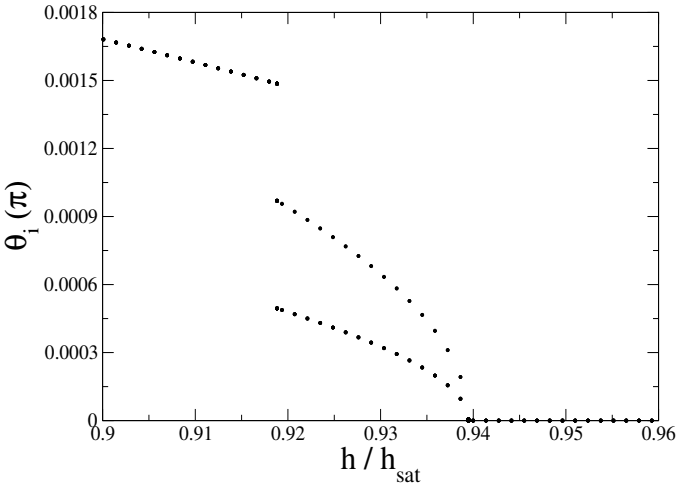


FIG. 14: Part of Fig. 9 in greater detail.

The projection of the total magnetization per spin along the field for the spins that participate in intermolecular bonds decreases across the discontinuities, with the exception of the jump that corresponds to the one of the isolated icosahedron (Figs 15 and 16). This was also the case for $N = 3$ (Sec. III). On the other hand, for the spins that only participate in intramolecular bonds this is the only jump that their corresponding projection decreases, unlike the $N = 3$ case, where there was no such decrease.

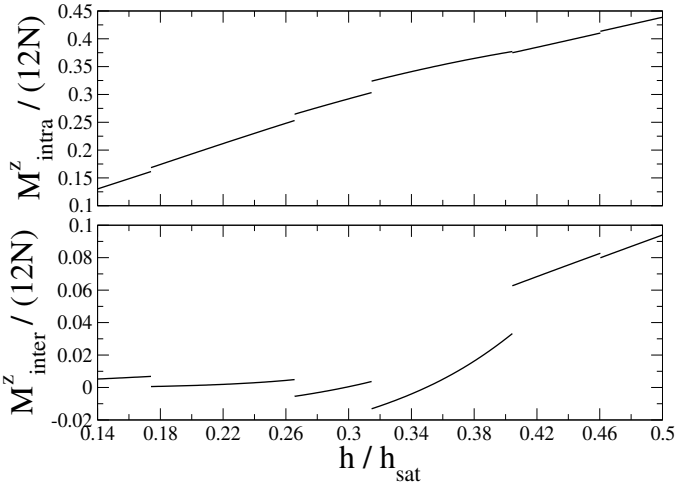


FIG. 15: Total magnetization per spin along the field of the spins that participate in intericosahedral bonds $M^z_{inter}$ and the ones that do not $M^z_{intra}$ as a function of the magnetic field over its saturation value $\frac{h}{h_{sat}}$ in the ground state of Hamiltonian (1) for a ring of $N = 6$ icosahedra for $\omega = \frac{\pi}{10}$.

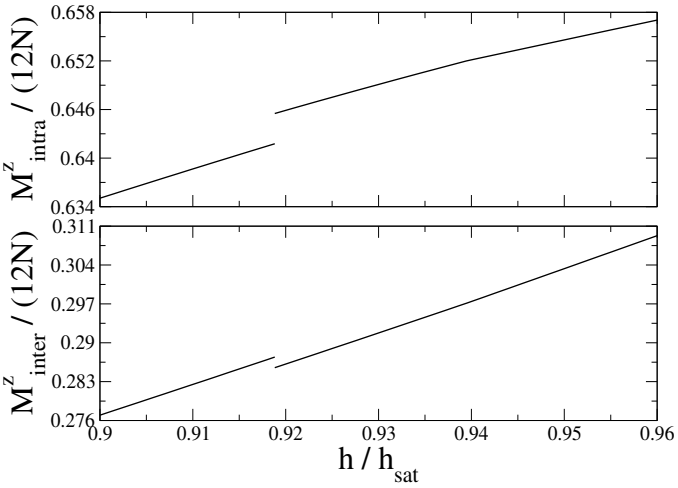


FIG. 16: Same as Fig. 15 but close to saturation.

## V. CONCLUSIONS

In this paper the classical magnetization response of rings of icosahedra was calculated with the antiferromagnetic spin interactions described by the AHM, which lacks any anisotropy. The magnetic response originates from the properties of an isolated icosahedron and the interactions between neighboring icosahedra. It is characterized by multiple magnetization discontinuities and lowest-energy configurations that have locally varying magnetization. For the three-membered ring the magnetization jump associated with the one of an isolated icosahedron appears at different magnetic fields for the different molecules of the ring. This results to an even more pronounced local variation of the magnetization and points to a difference in the magnetic behavior between even and odd-membered rings of molecules, similarly to what happens for rings of single spins.

It is of interest to consider larger rings, which will reveal how the magnetic response develops when going closer to the thermodynamic limit and what ground-state configurations develop in this case. However this is more demanding computationally. Another area of interest are structures of icosahedra that are more than one dimensional, going also in the direction of icosahedral quasicrystals and their approximants [34–38].


[1] A. Auerbach, *Interacting Electrons and Quantum Magnetism* (Springer Verlag, New York, 1998), ISBN 978-0-387-94286-5.

[2] P. Fazekas, *Lecture Notes on Electron Correlation and Magnetism* (World Scientific, Singapore, 1999), ISBN 978-981-02-2474-5.

[3] E. Manousakis, Rev. Mod. Phys. **63**, 1 (1991).

[4] C. Lhuillier and G. Misguich, *in High Magnetic Fields Applications in Condensed Matter Physics and Spectroscopy, Lecture Notes in Physics (Springer Series) Vol. 595, edited by C. Berthier, L. P. Levy, and G. Martinez (Springer, New York 2001).*

[5] G. Misguich and C. Lhuillier, *in Frustrated Spin Systems, edited by H.T. Diep (World Scientific, Singapore, 2003).*

[6] A. P. Ramirez, MRS Bull. **30**, 447 (2005).

[7] J. Schnack, Dalton Trans. **39**, 4677 (2010).

[8] Plato, *Timaeus.*

[9] H. Prinzbach, A. Weiler, P. Landenberger, F. Wahl, J. Wörth, L. T. Scott, M. Gelmont, D. Olevano, and B. v. Issendorff, Nature **407**, 60 (2000).

[10] Z. Wang, X. Ke, Z. Zhu, F. Zhu, M. Ruan, H. Chen, R. Huang, and L. Zheng, Phys. Lett. A **280**, 351 (2001).

[11] Z. Iqbal, Y. Zhang, H. Grebel, S. Vijayalakshmi, A. Lahamer, G. Benedek, M. Bernasconi, J. Cariboni, I. Spagnolatti, R. Sharma, et al., Eur. Phys. J. B **31**, 509 (2003).

[12] D. Vaknin and F. Demmel, Phys. Rev. B (R) **89**, 180411

(2014).
[13] L. Engelhardt, F. Demmel, M. Luban, G. A. Timco, F. Tuna, and R. E. P. Winpenny, Phys. Rev. B **89**, 214415 (2014).
[14] L. Qin, G.-J. Zhou, Y.-Z. Yu, H. Nojiri, C. Schröder, R. E. P. Winpenny, and Y.-Z. Zheng, J. Am. Chem. Soc. **139**, 16405 (2017).
[15] D. Coffey and S. A. Trugman, Phys. Rev. Lett. **69**, 176 (1992).
[16] N. P. Konstantinidis and D. Coffey, Phys. Rev. B **63**, 184436 (2001).
[17] H.-J. Schmidt and M. Luban, J. Phys. A: Math. and Gen. **36**, 6351 (2003).
[18] C. Schröder, H.-J. Schmidt, J. Schnack, and M. Luban, Phys. Rev. Lett. **94**, 207203 (2005).
[19] N. P. Konstantinidis, Phys. Rev. B **72**, 064453 (2005).
[20] N. P. Konstantinidis, Phys. Rev. B **76**, 104434 (2007).
[21] A. Hucht, S. Sahoo, S. Sil, and P. Entel, Phys. Rev. B **84**, 104438 (2011).
[22] J. Strečka, K. Karľová, and T. Madaras, Physica B **466-67**, 76 (2015).
[23] N. P. Konstantinidis, J. Phys.: Condens. Matter **28**, 016001 (2016).
[24] K. Karľová, J. Strečka, and T. Madaras, Physica B **488**, 49 (2016).
[25] K. Karľová, J. Strečka, and J. Richter, J. Phys.: Condens. Matter **29**, 125802 (2017).
[26] K. Karľová, J. Strečka, and T. Madaras, Acta Phys. Polon. A **131**, 630 (2017).
[27] N. P. Konstantinidis, SciPost Phys. **15**, 037 (2023).
[28] N. P. Konstantinidis (2022), cond-mat/2207.11077.
[29] N. P. Konstantinidis, J. Magn. Magn. Mater. **627**, 173061 (2025).
[30] D. P. Landau and K. Binder, Phys. Rev. B **24**, 1391 (1981).
[31] M. Holtschneider, S. Wessel, and W. Selke, Phys. Rev. B **75**, 224417 (2007).
[32] N. P. Konstantinidis, J. Phys.: Comm. **1**, 055027 (2017).
[33] N. P. Konstantinidis, J. Phys.: Condens. Matter **27**, 076001 (2015).
[34] D. Shechtman, I. Blech, D. Gratias, and J. W. Cahn, Phys. Rev. Lett. **53**, 1951 (1984).
[35] A. I. Goldman and R. F. Kelton, Rev. Mod. Phys. **65**, 579 (1993).
[36] S. Suzuki, A. Ishikawa, T. Yamada, T. Sugimoto, A. Sakurai, and R. Tamura, Mater. Trans. **62**, 298 (2021).
[37] A. P. Tsai, J. Q. Guo, E. Abe, H. Takakura, and T. J. Sato, Nature **408**, 537 (2000).
[38] R. Eto, M. Mochizuki, and S. Watanabe (2025), cond-mat/2502.11286.
[39] S. L. Altmann and P. Herzig, *Point-Group Theory Tables* (Oxford University Press, London, 1994), ISBN 978-0198552260.
[40] N. P. Konstantinidis, J. Phys.: Condens. Matter **28**, 456003 (2016).